Pressure effects on the magnetic-electronic behavior of the local moment ferromagnet CeCuSi

G R Hearne[1] , G Diguet[1], A M Strydom[1], B Sondezi-Mhlungu[1], K Kamenev[2], F Baudelet[3] , L Nataf [3]

[1] Department of Physics, University of Johannesburg , P.O. Box 524 , Auckland Park, 2006, Johannesburg, South Africa

[2] Centre for Science at Extreme Conditions (CSEC) and School of Engineering, University of Edinburgh, Edinburgh EH9 3JZ, United Kingdom

[3] Synchrotron SOLEIL, Saint-Aubin, 91192 Gif-sur-Yvette Cedex, France

E-mail : grhearne@uj.ac.za

Abstract. Magnetization measurements to ~10 GPa have been used to monitor both T_C and magnetic susceptibility in CeCuSi. The Ce valence and magnetic (5*d* moment) state to ~16 GPa at 6 K has been probed by means of L_3-absorption core-hole spectroscopy; in particular by X-ray absorption near edge spectroscopy (XANES) profiles and X-ray absorption dichroism (XMCD), respectively. Increasing pressure up to 10 GPa increases T_C from 15 K to 30 K. By contrast there is a decreasing XMCD intensity, signalling a collapsing Ce ordered moment. The XANES profiles show that the original $|4f^1>$ white line feature, typical of the localized 4*f* moment, diminishes at the expense of an emerging $|4f^0>$ (electron delocalization) component. The volume dependence of the hybridization between the 4*f* and *d* conduction-band states enhances the indirect exchange coupling between Ce ions and hence enhances T_C. However there is an attendant 4*f* level broadening resulting in a valence instability, which is disruptive to the stable configuration local moment situation prevailing at low pressure.

1. Introduction

Interest in Ce or U based ternary intermetallics has been ongoing for the last three decades, because they show a variety of exotic magnetic-electronic ground states (e.g., heavy fermion behavior, non-Fermi liquid effects, valence fluctuations, etc). Among the most intensively studied is the equiatomic Ce*TX* (*T* is a transition-metal, *X* is a *p* element) type compounds. Most magnetic Ce*TX* compounds order antiferromagnetically. One candidate, CeCuSi, is among a select number that rather exhibits ferromagnetic ordering at low temperatures; other candidates being CePdX (X = P, As, Sb) [1-3]. CeCuSi crystallizes in an ordered hexagonal ZrBeSi-type structure (space group $P6_3/mmc$, number 194) [3, 4]. The ferromagnetic transition in this compound has been established from both C_P specific heat data in which a λ-type anomaly is manifested at T_C =15 K and magnetization measurements in which an ordered moment of ~1 μ_B and stable configuration Ce^{3+} state has been obtained [3, 5, 6].

The hybridization between the localized *4f* and itinerant *d* electrons (Ce 5*d* and *T* 3*d*) is readily tuned (to increase) under pressure [7-9] . Consequently new ground states can be stabilized at reduced inter-atomic spacing without the complexity of disorder from doping. Many well known antiferromagnetic Ce*TX* compounds have been the focus of attention in pressure studies in the last

decade. There has been much less done, if any, in elucidating the pressure response of *ferromagnetic* analogs. This work reports on the magnetic-electronic pressure response of CeCuSi , using novel high pressure capabilities in diamond anvil high pressure cells (DACs).

SQUID magnetization pressure measurements of CeCuSi have been used to monitor the pressure evolution of both T_C and the susceptibility in the magnetically ordered state at $T < 15$ K. X-ray absorption spectroscopy (XAS) at the Ce L_3-edge (involving $2p \rightarrow 5d$ electronic transitions) is feasible under these stringent extreme conditions using specialized DAC methodology [10]. Therefore element specific X-ray absorption near edge spectroscopy (XANES) and X-ray magnetic circular dichroism (XMCD) measurements from these XANES spectra has been used to probe the Ce valence and its 5*d* moment (exchange coupled to the 4*f* moment), respectively; as implemented up to ~16 GPa at liquid helium temperatures.

2. Experimental

2.1. SQUID-magnetization pressure measurements

A miniature turn-buckle magnetic DAC (TM-DAC) [11] recently developed for magnetization studies in a small bore SQUID magnetometer (QD : MPMS), has been used for the magnetic pressure studies. This TM-DAC comprised of Cu-Be, with maximal pressure capabilities of 10 - 12 GPa, has sufficiently low background which is smoothly varying over a wide temperature range. Hence this can be readily subtracted from the measured DAC plus sample signal, to reliably reveal the magnetization details of the sample only. Diamond anvils with 800 μm culets have been used in the TM-DAC. The Cu-Be gasket has been pre-indented to a thickness of ~100 μm from a starting thickness of 250 μm and a cavity of ~400 μm diameter drilled in the center of the indention.

Well characterized homogeneous and single-phased polycrystalline CeCuSi from the same batch as previous studies has been used for these pressure experiments [4, 5]. A microscopic solid fragment of several μg of the CeCuSi sample was loaded into the cavity of the TM-DAC to ensure ~75 % filling factor. Tiny ruby chips were loaded alongside the sample for pressure determination from the ruby fluorescence [12]. Transparent Daphne 7373 mineral oil, sufficiently hydrostatic to several GPa has been used as pressure transmitting medium. The measurement protocol involved cooling the DAC in zero field to about 10 - 20 K above T_C , after which a 30 Oe field was applied and the magnetization (*M*) measured upon cooling the sample through the transition temperature region. At initial DAC closure the background corrected data revealed the same features of the transition as for the sample measured under ambient conditions outside of the DAC, confirming $T_C = 15$ K, see figure 1(a).

After unloading the DAC from the SQUID, pressure was increased and measured at room-temperature before commencing with the next *M-T* run at pressure. The pressures obtained from the ruby fragment loaded near the center of the cavity was typically within 5% of that of the ruby near the edge. Moreover, previous tests have indicated that when the TM-DAC is cooled to 2 K , there is a minimal change in pressure from the value locked in at room temperature [11].

2.2. XAS measurements

X-ray absorption measurements at the Ce L_3-edge (~5.7 keV) were performed at the energy-dispersive ODE (Optique Dispersive EXAFS) beamline of Synchrotron SOLEIL. An external field of 1.3 T has been applied along the beam path to impose a magnetization direction (i.e., orientations of majority and minority electron spin bands in the ferromagnet). The magnetic field is switched parallel and anti-parallel to the beam direction which is fully equivalent to changing the helicity of the photons incident on the sample. The dichroic signal (XMCD) is obtained from the difference between the (near edge) XANES spectra for two opposite directions of the external magnetic field.

The absorption of these incident photons at $L_{2,3}$ edges result in corresponding spin-polarized photoelectrons excited from 2*p* core levels, for "detecting" (i.e., populating) majority and minority

spin holes $N_h(m_s)$ in the Ce 5*d* conduction band above the Fermi level E_F ($2p \rightarrow 5d$ electric dipole transitions), where m_s is the electron spin quantum number [13].

Thus electron spin polarized X-ray absorption spectra (or spin dependent absorption coefficients) μ_+ and μ_- are recorded, from which the dichroism signal may be obtained (i.e., $\mu_+ - \mu_-$). A normalized spin-dependent absorption profile $(\mu_+ - \mu_-)/(\mu_+ + \mu_-)$ is computed from the absorption spectra so as to obtain the thickness-independent XMCD for comparison at various pressures.

The beam spot at the sample was 28 × 42 μm (FWHM). Energy calibration was by means of a $CeFe_2$ reference sample [14]. Pressurization involved an in-house membrane-DAC assembly cooled to ~6 K in a closed-cycle cryogenic system and pressure adjusted "on-line" at the desired temperature. Perforated diamond anvil methodology was employed; imperative for the high gains in transmission desirable at the ~5.7 keV L_3-edge where there is considerable absorption (> 95 %) by conventional diamond anvils. This arrangement entailed mounting miniature diamond anvils of 500 μm thickness on bigger diamonds serving as backing plate supports through which holes had been laser drilled.

Powdered sample was loaded into the confining cavity (diam. ~80 μm) drilled in an inconel gasket pre-indented to a final thickness of ~ 20 μm. Silicone oil was loaded as an appropriate pressure transmitting medium. Pressure values were determined using the ruby fluorescence method, from ruby balls loaded in the cavity. Pressure was initially set at room temperature and after the DAC had been cooled to ~6 K the pressure was again checked in-situ in the beamline for drift.

3. Results and discussion

3.1 Magnetization measurements

Figure 1(a) shows that the precipitous step change in the magnetization typically occurring at the spin alignment transition (T_C) diminishes upon rising pressure, until such transition signatures are considerably reduced at ~10 GPa. The T_C (midpoint) increases monotonically from 15 K at ambient pressure up to ~30 K at 10 GPa (figure 1(b)). This behavior is nearly replicated by T_C (onset) and shows that spin correlations are onset well above 30 K at the highest pressures. The magnetic susceptibility of the spin aligned state (low field magnetization value at ~9 K, figure 1(c)) decreases non-monotonically and extrapolates to the paramagnetic baseline in the range 10 – 15 GPa. This contrasting behavior of increasing T_C yet collapsing magnetic susceptibility as a function of pressure merits deeper investigation, e.g., of how the pertinent Ce electronic state is responding under pressure at $T << T_C$. Therefore element specific XANES and its dichroism (XMCD) at the Ce L_3-edge under these stringent extreme conditions is considered appropriate (and is perhaps the only means) to directly monitor the Ce valence and probe the Ce moment, respectively.

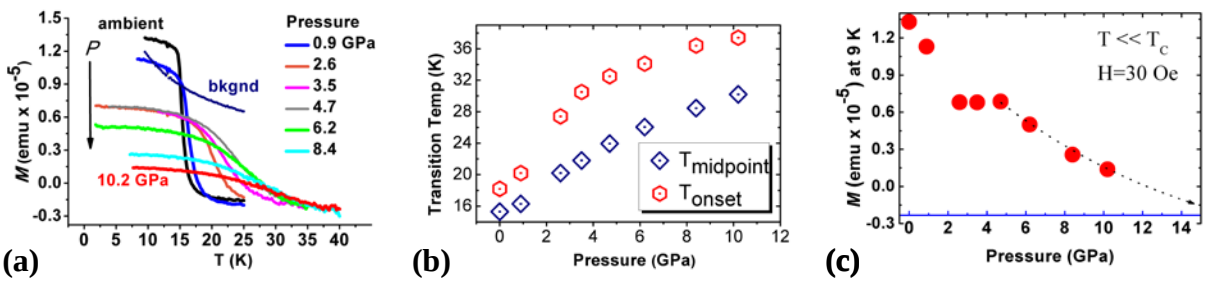

Figure 1 (color online): (a) Background subtracted magnetization-temperature curves as a function of increasing pressure. (b) Pressure evolution of T_C and (c) low field magnetization (susceptibility) at 9 K .

3.2 XANES and XMCD results

L_3-absorption is a core-hole spectroscopy based on the excitation of 2*p* core electrons into 5*d* valence orbitals. Sensitivity to the 4*f* electrons arises through *d–f* hybridization and the intra-atomic 4*f* - 5*d* magnetic exchange interaction. The different components of the Ce electronic ground state, i.e., $|4f^0\rangle$ (itinerant), $|4f^1\rangle$ (localized) and $|4f^2\rangle$ (strong hybridization with conduction electrons), make different contributions in the XANES spectrum. This is because the energy attributed to each $|4f^i\rangle$ final state configuration in the $2p \rightarrow 5d$ transition is different, due to their respective screening effects on the 2*p* core hole. For example, in the final state either the core hole is well screened by a 4*f* electron ($|4f^1\rangle$ localized configuration) yielding the low-energy structure at the L_3 edge (so called "white line") or is poorly screened by the 5*d* conduction band electron ($|4f^0\rangle$ itinerant configuration), the latter giving rise to a white line feature at higher energies (6 – 10 eV) from the $|4f^1\rangle$ peak. The effect of a $|4f^2\rangle$ configuration is more difficult to discern and usually occurs as a low intensity peak in the pre-edge region, where it is masked by core-hole lifetime broadening effects of the $|4f^1\rangle$ main white line [10]. Relative intensities of these spectral features may be used to establish the ground state admixture $c_0|4f^0\rangle + c_1|4f^1\rangle$ [10, 14], where $(c_i)^2$ represents the weight of the individual electronic configurations. The fractional 4*f* occupation number n_f may be obtained from relative intensities of the $4f^0$ and $4f^1$ contributions in the XANES profile, $n_f = (c_1)^2/[(c_1)^2+(c_0)^2]$ [14]. Such an estimation sets an upper limit on n_f, as the contribution from $|4f^2\rangle$ is not accessible and therefore $(c_2)^2$ is not included. The case of $n_f < 1$ (non-integral 4*f* occupation) signifies a mixed valence or valence fluctuating state of Ce in the compound, that is , electron delocalization.

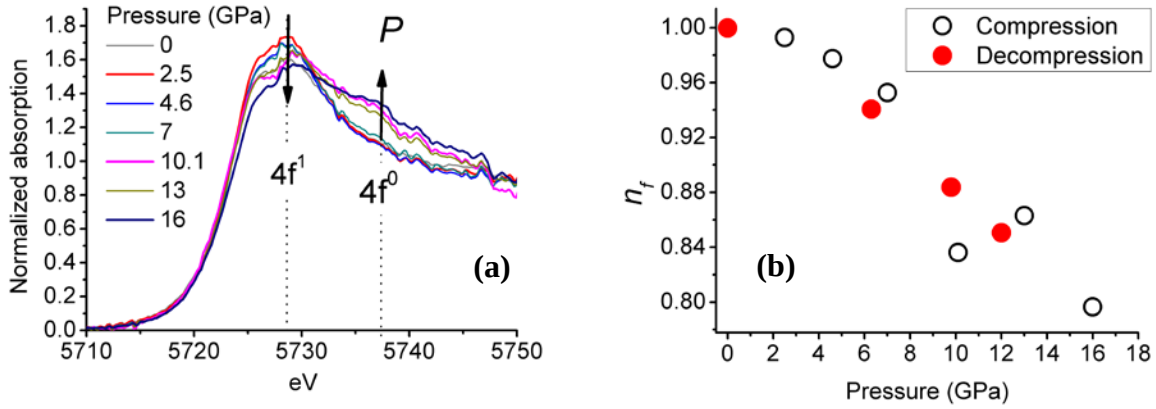

Figure 2 (color online) : (a) Pressure evolution of the XANES profiles at 6 K, upon compression. The positions of the $|4f^0\rangle$ and $|4f^1\rangle$ features have been delineated. (b) The 4*f* level occupancy n_f as estimated from $|4f^0\rangle$ and $|4f^1\rangle$ white lines in the XANES, both for compression and decompression sequences. This is normalized to the assumed full occupancy, Ce^{3+}, in the stable configuration state at ambient pressure.

Figure 2(a) depicts the evolution of the XANES profiles as a function of pressure. These have been normalized to an edge jump of unity. Near ambient pressure the spectrum exhibits a pronounced single white line feature, attributed to the $|4f^1\rangle$ final state configuration anticipated for this local moment ferromagnet. As pressure increases this white line intensity decreases and an additional white line intensity at about 10 eV higher in energy evolves. This hump feature, characteristic of the $|4f^0\rangle$ configuration [10], grows as a function of pressure at the expense of the $|4f^1\rangle$ intensity. The transfer of spectral weight from the $|4f^1\rangle$ to $|4f^0\rangle$ component, conspicuously evident at $P \geq 10$ GPa in figure 2(a), provides here experimental evidence of the 4*f* electron delocalization under pressure. This is representative of a progressive valence transition from Ce^{3+} at ambient pressure [6], towards Ce^{4+}.

The obvious decrease in 4*f* level occupancy plotted in figure 2(b) also exemplifies this electron delocalization. Furthermore the electronic transition is reversible with the stable-configuration state being re-attained upon decompression back to ambient pressure.

The valence instability impacts on the magnetic moment of the Ce ion. This is monitored by the XMCD, obtained from the difference between the XANES profiles associated with right and left circularly polarized incident photons as described in section 2.2. The imbalance of 5*d* unoccupied states in the majority and minority spin channels are probed. The XMCD thus probes the ordered moment (spin and orbital) contribution derived from the 5*d* exchange split majority and minority spin bands [13]. This exchange splitting (relative shift of 5*d* spin-up and down bands) has its origin in the *intra-atomic exchange* field from (i.e., magnetic coupling to) the ordered Ce 4*f* moment [15] , as derived from the electronic ground state $c_0|4f^{\,0}\rangle + c_1|4f^{\,1}\rangle$. Monitoring the L_3-edge XMCD and associated 5*d* moment is therefore a means of tracking the behavior of the ordered Ce 4*f* moment. Figure 3 shows that there is a monotonically decreasing XMCD intensity as pressure increases, indicative of a collapsing Ce 5*d* ordered moment contribution.

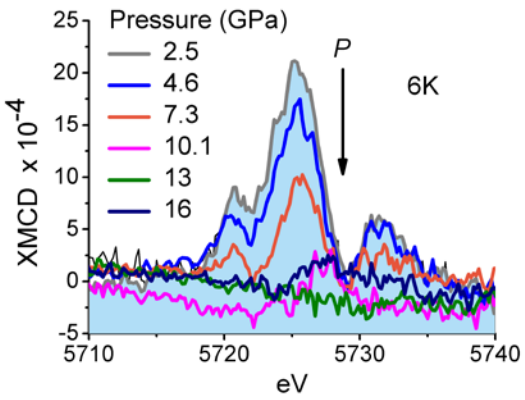

Figure 3 (color online) : XMCD signal (normalized to the absorption edge jump) upon increasing pressure. Signal intensity is proportional to the Ce 5*d* moment contribution. Collapse of the signal is evident at $P \geq 10$ GPa. The intensity is reconstituted upon decompression to ambient pressure, i.e., reversibility obtains as in figure 2(b).

3.3 Discussion

The 4*f* electrons are highly localized and Ce inter-site distances are comparatively much larger. Magnetic coupling between Ce local moments, responsible for spin alignment and the T_C energy scale, is through an *indirect exchange* mechanism involving polarization of the *d* conduction band electrons; the Ruderman-Kittel-Kasuya-Yosida (RKKY) interaction. The RKKY exchange coupling strength $J_{d\text{-}f}$ depends on the hybridization between the (Ce) localized 4*f* electron states with those *d* band (Cu 3*d* and Ce 5*d*) electronic states of comparable energy [9]. The dependence of T_C on $J_{d\text{-}f}$ in stable configuration local moment Ce compounds is expected to behave as $T_C \propto (J_{d\text{-}f})^2 \times N(E_F)$, where $N(E_F)$ is the density of states at the Fermi energy. The application of pressure generally leads to an increase in the product $|J_{d\text{-}f}\, N(E_F)|$ in such stable configuration systems [9]. This is attributable to the dependence of $J_{d\text{-}f}$ on the *d-f* orbital hybridization $V_{d\text{-}f}$ [8]:

$$J_{d-f} \propto \frac{-2}{E_F - \varepsilon_f}\left[\frac{r_f^5 r_d^3}{R^{12}}\right] \qquad (1)$$

where ε_f is the energy of the 4*f* level considered to be pinned close to the Fermi level E_F. The term in square brackets, proportional to $|V_{d\text{-}f}|^2$, is seen to have strong dependences on the atomic radii *r* of 4*f* (Ce) and 3*d* (Cu) atoms as well as their inter-atomic separation *R*. This emphasizes that the RKKY exchange $J_{d\text{-}f}$ would have a pressure dependence, via the inter-atomic spacing dependence of the *d-f* hybridization in $|V_{d\text{-}f}|^2$ [8, 16]. The increase in T_C in figure 1 as pressure increases is therefore ascribed to the increased *d-f* hybridization as *R* is reduced under pressure.

However, the XANES data of figure 2 suggests progressive delocalization of the 4*f* electron occurs upon increasing pressure. This is compatible with increased *d-f* hybridization which additionally leads to broadening of the 4*f* level (i.e., ε_f in equation 1)) related to such delocalization. Increased partial delocalization is disruptive to the local moment character of the stable configuration Ce^{3+} valence ($|4f^1>$), prevalent in CeCuSi at low pressure [6]. The decrease in magnetic susceptibility in the ordered state in figure 1(c) is thus ascribed to this increasing partial delocalization. XMCD data of figure 3 appears to corroborate this suggestion : notably that the Ce 5*d* moment, resulting from the 4*f*-5*d intra-atomic exchange* (thus tracking the 4*f* moment) [15], exhibits a progressive diminution as a function of pressure as well.

4. Concluding remarks

In the stable configuration local moment situation at low pressure in CeCuSi , the effect of reducing the unit cell volume beneficiates the RKKY exchange coupling $J_{d\text{-}f}$ between Ce moments as mediated by *d* conduction electrons. This is exhibited in the monotonically increasing T_C upon pressurization. Increasing *d-f* hybridization in the relation $J_{d\text{-}f} \propto |V_{d\text{-}f}|^2$ and its strong dependence on inter-atomic spacing between Ce 4*f* and Cu 3*d* atoms rationalizes this enhancement of T_C. On the other hand, the increase in $V_{d\text{-}f}$ consequentially broadens the original 4*f* localized level (i.e., band formation occurs). Thus sufficient 4*f* electron delocalization occurs, as seen by L_3-edge XANES, to the extent that it disrupts the Ce^{3+} stable-configuration moment, $|4f^1>$, as probed by the L_3-edge dichroism.

Acknowledgements

Project funding derived from NRF (CPRR) and UJ (URC) grants as well as the loan of the perforated-anvils membrane-DAC assembly from Dr J-P Itie´ (SOLEIL) , is acknowledged with gratitude.

References

[1] Trovarelli O, Sereni J G, Schmerber G and Kappler J P 1994 *Phys. Rev. B* **49** 15179-83
[2] Katoh K, Takabatake T, Ochiai A, Uesawa A and Suzuki T 1997 *Physica B* **230** 159-61
[3] Yang F, Kuang J P, Li J, Brück E, Nakotte H, Boer F R d, Wu X, Li Z and Wang Y 1991 *J. Appl. Phys* **69** 4705 - 7
[4] Sondezi-Mhlungu B M, Adroja D T, Strydom A M, Paschen S and Goremychkin E A 2009 *Physica B* **404** 3032 - 4
[5] Sondezi-Mhlungu B M, Adroja D T, Strydom A M, Kockelmann W and Goremychkin E A 2010 *Journal of Physics: Conference Series* **200** 012190 (1 - 4)
[6] Gignoux D, Schmitt D and Zerguine M 1986 *Solid State Comm.* **58** 559 - 62
[7] Süllow S, Aronson M C, Rainford B D and Haen P 1999 *Phys. Rev. Lett.* **82** 2963 - 6
[8] Cornelius A L and Schilling J S 1994 *Phys. Rev. B* **49** 3955 - 61
[9] Schilling J S 1979 *Adv. in Phys.* **28** 657-715
[10] Rueff J-P, Raymond S, Taguchi M, Sikora M, Itie´ J-P, Baudelet F, Braithwaite D, Knebel G and Jaccard D 2011 *Phys. Rev. Lett.* **106** 186405 (1 - 4)
[11] Giriat G, Wang W, Attfield J P, Huxley A D and Kamenev K V 2010 *Rev. Sci. Instrum.* **81** 073905 (1-5)
[12] Chijioke A, Nellis W J, Soldatov A and Silvera I F 2005 *J. Appl Phys.* **98,** 114905 (1 - 9)
[13] Stöhr J and Siegmann H C 2006 *Magnetism: From Fundamentals to Nanoscale Dynamics* vol 152 (Berlin: Springer)
[14] Giorgetti C, Pizzini S, Dartyge E, Fontaine A, Baudelet F, Brouder C, Bauer P, Krill G, Miraglia S, Fruchart D and Kappler J P 1993 *Phys. Rev. B* **48** 12732 - 42
[15] Parlebas J C, Asakura K, Fujiwara A, Harada I and Kotani A 2006 *Phys. Rep.* **431** 1 - 38
[16] Harrison W A 1983 *Phys. Rev. B* **28** 550 - 9